Kerbala Journal of Veterinary Medical Sciences Issue (2), Volume (2), (2026)

Chronic Iodine-Induced Histological Alterations in the Cerebral Cortex and Liver of Guinea Pigs

Bushra Faleh, Muna Hussain

Department of Anatomy and histology, College of Veterinary Medicine, University of Kerbala, Kerbala, Iraq
Corresponding author: bushra.faleh@s.uokerbala.edu.eq

Received:15/5/2026 **Accepted:** 26/5/2026 **Published:** 15/6/2026

***Abstract*—** Iodine is a double-edged sword; while essential for thyroid function, excessive intake triggers systemic toxicity. This study evaluated the chronic effects of oral iodine on the liver and brain of thirty guinea pigs over a 60-day period. The animals were divided into: Group I (Negative Control); Group II (Positive Control, receiving potassium iodide at 10 mg/kg); and Group III (Experimental, receiving a 20% iodine solution). The study utilized biochemical assays, H&E staining, and Nissl staining to assess cellular and neuronal integrity. Hepatotoxicity and Metabolic Impairment Biochemical analysis revealed a significant, time-dependent elevation in serum ALT and AST levels, particularly in Group III. Neuro histological Changes and Neuronal Degeneration The central nervous system showed marked vulnerability to chronic iodine exposure, Meningeal vascular congestion, liquefactive cortical necrosis, diffuse neuronal death, and reactive astrogliosis were observed in histopathological analysis of treated animals. Nissl staining additionally showed prominent chromatolysis, consistent with loss of neuronal protein synthesis. The chronic overexposure to iodine precipitates irreversible multi-organ dysfunction by cellular necrosis and metabolic perturbation, with the severity of toxicity being highly dose-dependent and therefore requiring the establishment of strict evidence-based upper intake limits.

Keywords **—** Iodine toxicity, Nissl staining, Neurodegeneration, Guinea pigs, liver toxicity, PAS.

INTRODUCTION

Iodine is a vital micronutrient involved in the biosynthesis of thyroid hormones, which are essential for normal metabolic activity, growth, and neurodevelopment. Maintaining iodine balance is critical for physiological homeostasis, as both deficiency and excess can adversely affect health. While iodine deficiency has been extensively studied, increasing evidence suggests that histological and functional alterations, particularly within the central nervous system (1,2)

"The liver is the primary organ responsible for thyroid hormone metabolism; therefore, elevated thyroid hormone levels may lead to complex effects on liver function and hepatic enzymes (3).

The histological changes in the liver indicated toxic effects characterized by hepatocyte necrosis, nuclear fragmentation and dissolution, as well as cellular degeneration with cytoplasmic vacuolation and ballooning degeneration. The severity of these alterations was dose- and time-dependent (4) The liver is a vital organ with essential roles in metabolism, glycogen storage, and detoxification processes. Evaluation of its structural and functional integrity is commonly performed using histological staining techniques.

The central nervous system is particularly vulnerable to toxic and metabolic disturbances, as neuronal cells are highly sensitive to factors that impair protein synthesis and cellular homeostasis (5,6). Nissl bodies, which represent the rough endoplasmic reticulum within the neuronal cytoplasm, play a crucial role in protein synthesis and maintenance of neuronal function (7). Therefore, alterations in Nissl substance are considered important histological markers of neuronal injury, and Nissl staining is widely employed as a reliable method for detecting early neurodegenerative changes (8).

Despite the essential physiological role of iodine, limited studies have investigated its chronic effects on brain tissue, particularly at the histological level using Nissl staining, and the extent of its associated systemic histopathological alterations remains insufficiently understood (9). Moreover, prolonged iodine exposure may induce structural changes not only in neural tissue but also in other organs, reflecting its potential systemic toxicity. Therefore, the present study was designed to evaluate the chronic effects of iodine exposure on brain tissue in guinea pigs, with particular emphasis on neuronal alterations using Nissl staining, alongside histological assessment of the liver and skin using hematoxylin and eosin (H&E) staining over a 60-day exposure period. Histologically, the guinea pig brain provides a suitable model for such investigations due to its well-defined anatomical organization (10). The brain is relatively small, whitish in color, and globular in shape, consisting of the cerebrum, cerebellum, and brainstem. The cerebral cortex is characterized by distinct histological layers, including the pyramidal, plexiform, and granular layers, which differ in thickness and cellular density, while the cerebellum exhibits a comparable structural organization (11).

MATERIALS AND MTHODS

1. Experimental Animals and Ethical Considerations

Thirty healthy adult male guinea pigs (body weight: 500 \pm 50 g) were utilized for this study. The animals were acclimated in a controlled laboratory environment maintained at a constant temperature of 22 \pm 2^\circ\text{C} with a regulated 12-hour light/dark cycle. They were provided with a standardized pellet diet and water ad libitum.

Ethical Approval: All experimental protocols and animal handling procedures were strictly reviewed and approved by the Institutional Animal Care and Use Committee (IACUC) at [University of Karbala's College of Veterinary Medicine] (Approval No. [UOK.VET.AN.2025.142]). The study adhered to the internationally recognized guidelines for the care and use of laboratory animals, such as the NIH Guide. Every measure was taken to minimize animal distress and optimize the number of subjects used.

2. Preparation of Iodine Solution and Dosage Rationale

A 20% (w/v) iodine stock solution was prepared by dissolving iodine crystals in distilled water, utilizing potassium iodide as a stabilizing and solubilizing agent. The experimental dosage was determined based on a preliminary LD50 (median lethal dose) pilot study (12). A threshold of 200 mg/kg of body weight was established for the treatment groups, administered daily via oral gavage to investigate systemic toxicity over a chronic duration.

3. Experimental Design and Grouping

The subjects were randomly assigned into three experimental cohorts (n=10 per group):

- Group I (Negative Control): Administered distilled water only.
- Group II (Positive Control): Administered potassium iodide to differentiate compound-specific effects.
- Group III (Iodine Treatment): Administered the 20% iodide solution at a dosage of 200 mg/kg) (12).

To evaluate the temporal progression of iodine-induced pathology, a longitudinal sampling design was implemented. Animals from each group were humanely sacrificed at three specific time intervals: Day 20, Day 40, and Day 60.

Prior to sacrifice, animals were anesthetized, and blood samples were collected via cardiac puncture for biochemical profiling. Immediately following euthanasia, liver and brain tissues were harvested and fixed in 10% neutral buffered formalin for 24 hours to preserve morphological integrity.

4. Biochemical and Histological Analysis

Biochemical Assays: Serum was isolated from blood samples via centrifugation at 3000 rpm for 10 minutes. The activity of liver-specific enzymes, specifically Alanine Aminotransferase (ALT) and Aspartate Aminotransferase (AST), was quantified using commercial diagnostic kits.

Histological Processing: Following fixation, tissues underwent automated processing, including dehydration in a graded ethanol series, clearing in xylene, and embedding in paraffin wax. Serial sections were cut at a thickness of 5\ \mu\text{m} and subjected to the following staining protocols:

1. Hematoxylin and Eosin (H&E): For the assessment of general architectural and morphological alterations.
2. Periodic Acid–Schiff (PAS): To quantify hepatic glycogen reserves and metabolic status.
3. Nissl Staining: To evaluate neuronal cytological integrity and the density of Nissl substance.

STATISTICAL ANALYSIS

Microscopic evaluation was performed using a light microscope coupled with a high-resolution digital imaging system. Quantitative biochemical data were subjected to Two-way Analysis of Variance (ANOVA) using [GraphPad Prism 9.0] to compare differences across groups and time points. Data are presented as Mean ± Standard Error (Mean ± SE), with statistical significance defined at $P < 0.05$.

RESULT AND DISCUSSION

Normal hepatic and neuronal histoarchitecture, physiological AST/ALT levels (Fig.1), well organized hepatic lobular structure with abundant PAS positive glycogen granules in hepatocyte cytoplasm and bile duct epithelium, while preserved pyramidal and Purkinje cell morphology with closely packed Nissl granules indicative of active protein synthesis (Fig. 2,3). Progressive iodine exposure induced time-dependent impairment in both organs. Mild transaminase elevation as evidence of early hepatocellular membrane stress (significantly increased ALT activity followed by slight increase in AST), moderate decrease in glycogen content and partial bile duct PAS diminution were observed at 20 days (Fig. 4,5), and an initial assessment of Purkinje cell cytoplasmic stress while Nissl staining remains visible (Fig. 6.7). At 40-days both AST/ALT elevations and reductions in glycogen were most severe, resulting in reduced bile duct staining (Fig. 8,9), simultaneous with progressive reduction of Nissl substance and the appearance of early rough endoplasmic reticulum disruption in the Purkinje cell (Fig. 10,11). Severe hepatocellular damage was confirmed at day 60 by prominent transaminase elevation, almost complete loss of PAS reactivity in liver parenchyma, and pronounced lobular architectural disruption (Fig. 12,13) and dramatic neurodegeneration with pronounced chromatolysis and striking capitulation in neuronal protein synthesis indicates advanced multi-organ toxicity due to iodide (Fig. 14,15).

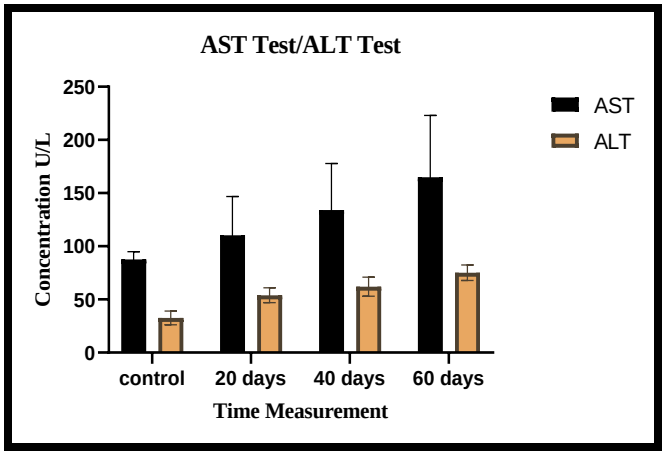

Figure 1. The chart compares the concentration levels of AST and ALT enzymes across four measurement periods: control group, 20 days, 40 days, and 60 days.

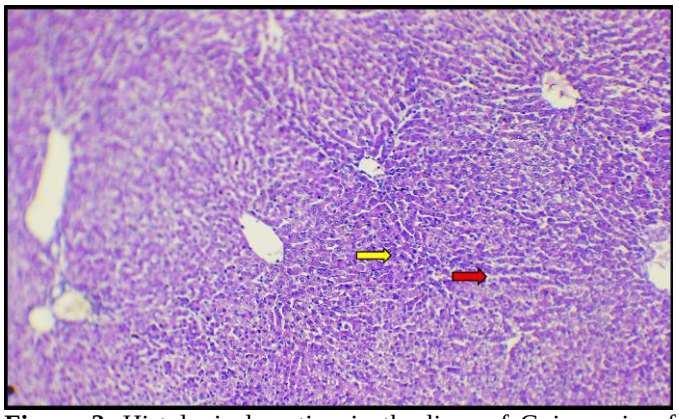

Figure 2. Histological section in the liver of Guinea pig of control group shows regular architecture of hepatic cord from the central vein composed of hepatocytes) yellow arrow) with sinusoids between hepatocytes cords (red arrow) (H&E stain 10,40 X)

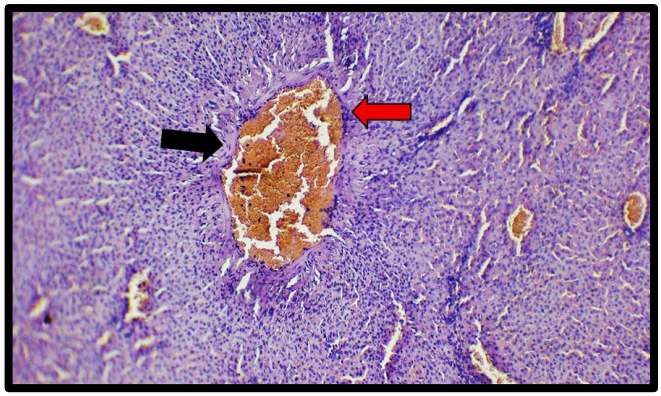

Figure 3. Histological section in the liver of Guinea pig of treated group at 20 days shows vascular congestion with peri vascular fibrosis (black arrow) perivascular mononuclear cells infiltration (red arrow) H&E stain(40X).

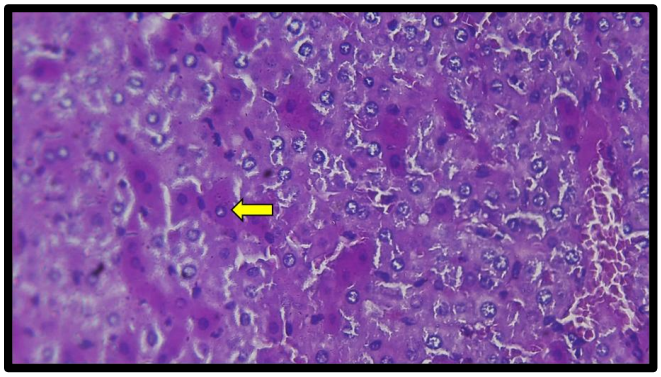

Figure 4. Histological section in the liver of Guinea pig of treated group at 20 days shows moderate PAS reaction that purple-red within cytoplasm of hepatocytes representing stored glycogen distributed throughout hepatic lobules with dark blue nuclei (yellow arrow) PAS stain (40 X).

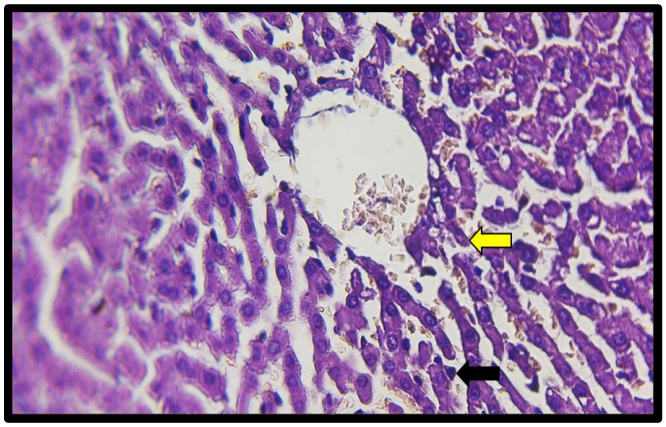

Figure 5. Histological section in the liver of Guinea pig of treated group at 40 days shows irregular architecture of hepatic cord sever (yellow arrow) with proliferation of Kupffer cells (black arrow) H&E stain (40 X).

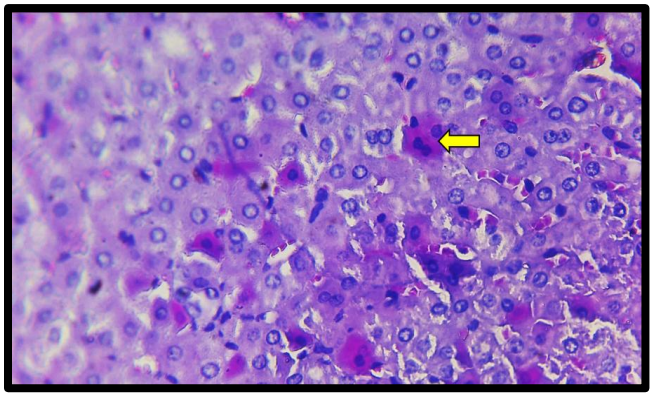

Figure 6. Histological section in the liver of Guinea pig of treated group at 40 days shows mild PAS reaction that purple-red within cytoplasm of hepatocytes representing stored glycogen distributed throughout hepatic lobules with dark blue nuclei (yellow arrow) PAS stain (40 X)

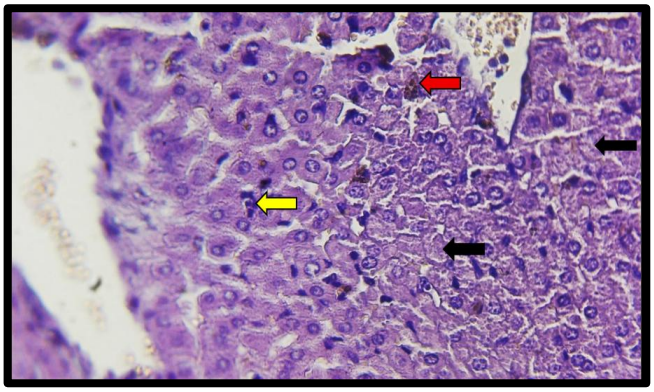

Figure 7. Histological section in the liver of Guinea pig of treated group at 60 days shows deposition of brown piment in the cytoplasm of hepatocytes (red arrow) with sever necrosis that nuclear karyolysis (black arrow) with leukocytic cells infiltration in the sinusoids (yellow arrow) H&E stain (40 X**)**

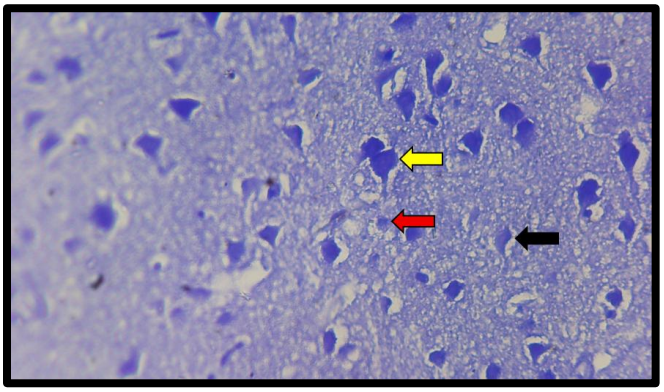

Figure 10. Histological section in the brain of Guinea pig of control shows dark blue granules within the cytoplasm of neurons (yellow arrow) with pale cytoplasm within glial (red arrow) and epithelial cells (black arrow) in the nervous tissue Nissl stain (40 X).

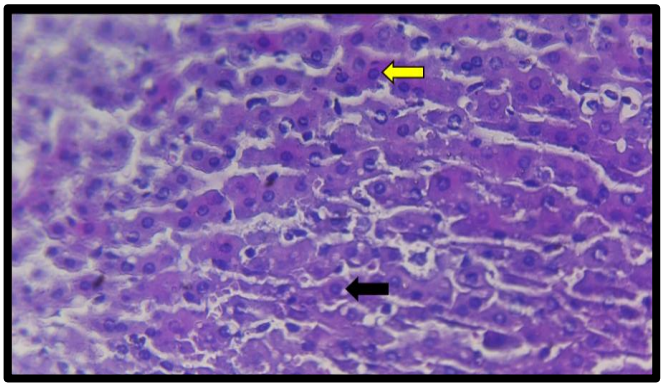

Figure 8. Histological section in the liver of Guinea pig of treated group at 60 days shows reduction (yellow arrow) or complete loss (black arrow) of PAS-positive glycogen granules within cytoplasm of hepatocytes (yellow arrow) PAS stain (40 X).

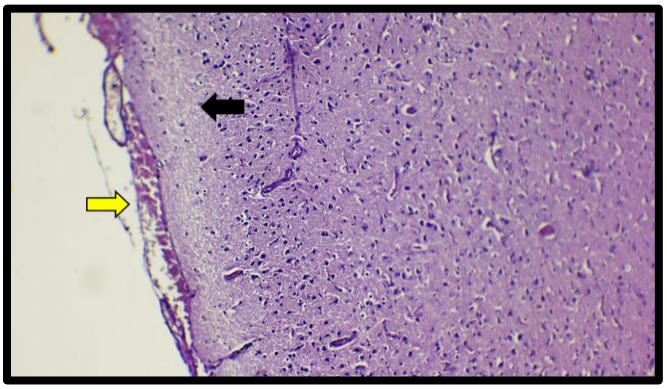

Figure 11. Histological section in the brain of Guinea pig of treated group at 20 days shows congestion of meningeal blood vessels (yellow arrow) with liquefactive necrosis in the cerebral cortex (black arrow) H&E stain (10X)

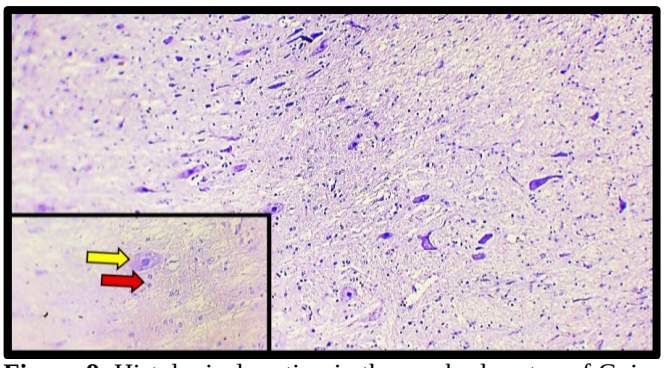

Figure 9. Histological section in the cerebral cortex of Guinea pig of control group shows basophilic cytoplasm of the Purkinje cells (yellow arrow) with bundles of thick nerve fibers originating in the presence of glial cells (red arrow) (H&E stain 10,40X).

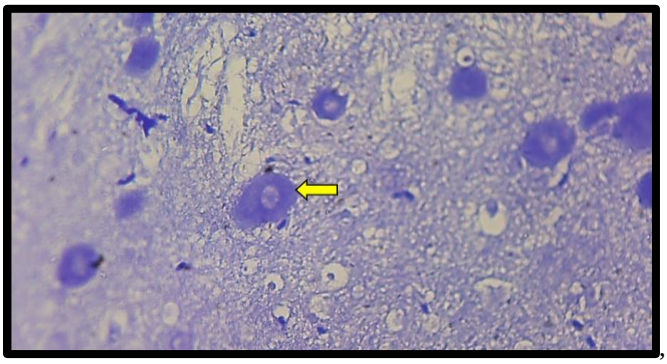

Figure12. Histological section in the brain of Guinea pig of treated group at 20 days shows moderate reaction for the cytoplasm of Purkinje cells that stain blue color (yellow arrow) Nissl stain (40 X).

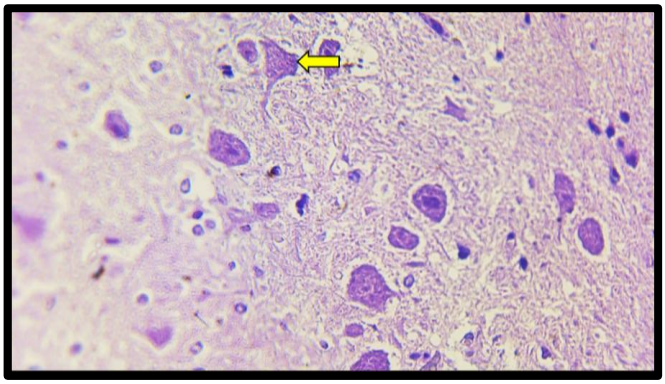

Figure 13. Histological section in the brain of Guinea pig of treated group at 40 days shows degeneration & necrosis of Purkinje cells in the granular layer (yellow arrow) (40 X).

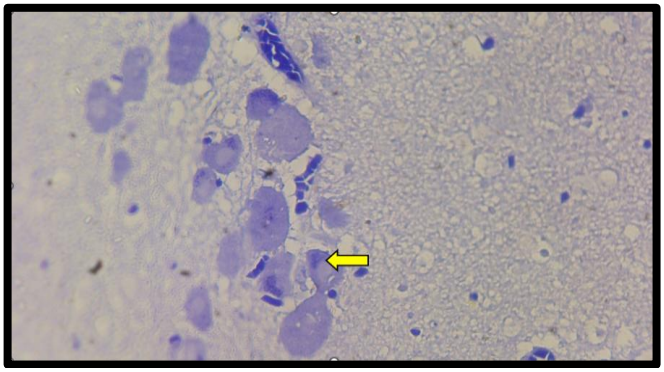

Figure 14. Histological section in the brain of Guinea pig of treated group at 40 days shows mild reaction for the cytoplasm of Purkinje cells that stain blue color (yellow arrow) Nissl stain (40 X).

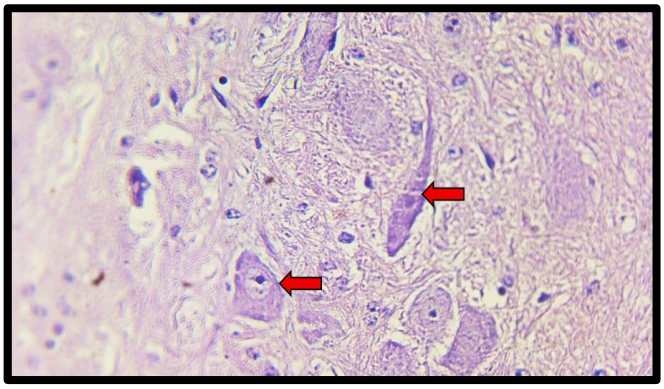

Figure 15. Histological section in the brain of Guinea pig of treated group at 60 days shows sever necrosis of Purkinje cells (red arrow)) H&E stain (40 X).

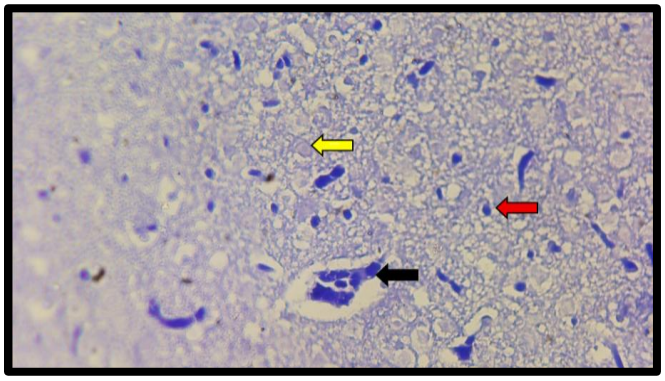

Figure 16. Histological section in the brain of Guinea pig of treated group at 60 days shows weak rection for pale or unstained granules within the cytoplasm of neurons (yellow arrow) with strong reaction for dark blue cytoplasm within glial (red a narrow) & blood vessel (black arrow) (Nissl stain (40 X).

Discussion

The elevation of AST and ALT observed in the present study may be attributed to hepatocellular damage induced by iodine toxicity, resulting in leakage of intracellular enzymes into the bloodstream due to membrane disruption and hepatocyte necrosis (13). Histopathological examination supported the biochemical results. At early stages (20 days), mild degenerative changes and moderate reduction in PAS-positive glycogen were observed, indicating early metabolic disturbance. At 40 days, inflammatory cell infiltration, sinusoidal dilation, and focal hepatocellular necrosis became prominent, accompanied by marked depletion of glycogen stores. At the terminal stage (60 days), severe hepatocellular necrosis, leukocytic infiltration, and pigment deposition were evident, along with near complete loss of PAS-positive material, suggesting severe impairment of carbohydrate metabolism (14). Masson trichrome staining further indicated increased collagen deposition at late stages, suggesting early fibrotic changes, which may represent a chronic response to continuous toxic exposure (15). These findings are in agreement with previous reports describing that persistent toxic insult leads to progressive hepatic degeneration, inflammation, and fibrosis (16,17). Overall, the combined biochemical and histological alterations confirm that iodine exposure induces significant hepatotoxic effects characterized by oxidative stress, metabolic disruption, and structural liver damage (18). The present study demonstrated that chronic iodine exposure induces progressive histological alterations in the brain tissue of guinea pigs, as evidenced by the gradual changes in Nissl staining intensity (19,20). These findings suggest that prolonged iodine administration may exert neurotoxic effects on neuronal integrity in a time-dependent manner (21). In the control group, the presence of well-defined and intensely stained Nissl granules reflects normal neuronal metabolic activity and active protein synthesis (22). Since Nissl bodies are essential for the synthesis of proteins required for neuronal maintenance and function, their structural integrity is considered an important indicator of neuronal health and viability (23). In contrast, following iodine exposure, a progressive reduction in Nissl staining

intensity was observed over the experimental periods (20, 40, and 60 days). Initially, the moderate reaction detected at 20 days may represent an adaptive or early cellular response to toxic insult. However, the subsequent mild and weak reactions observed at 40 and 60 days indicate a progressive reduction in Nissl substance (chromatolysis), which is commonly associated with neuronal stress, injury, or degeneration (9,24,25). Moreover, this decline in staining intensity suggests impaired protein synthesis within neurons, particularly in Purkinje cells, which are highly sensitive to toxic and metabolic disturbances. This impairment may be attributed to oxidative stress, metabolic disruption, or the direct cytotoxic effects of iodine on neuronal cells, all of which can compromise neuronal survival and function (25,26).

Furthermore, the progressive nature of these alterations supports the concept of a time-dependent neurotoxic effect of iodine, whereby longer exposure results in greater tissue damage (27). Importantly, these findings are consistent with previous studies reporting that prolonged exposure to toxic substances leads to neuronal degeneration and a marked reduction in Nissl substance further confirming the vulnerability of neuronal tissue to chronic toxic insults (28).

Conclusion

In conclusion, the study demonstrated that chronic iodine exposure induced significant histological alterations in both liver and brain tissues. In the liver, PAS staining revealed changes in glycogen content and impaired metabolic activity of hepatocytes, while in the brain, a progressive reduction in Nissl granules and decreased staining intensity in Purkinje cells were observed. These findings indicate time-dependent cellular damage and functional disturbances associated with prolonged iodine administration.

REFERENCES

1) Gottardi, W. (2001). Iodine and iodine compounds. *Disinfection, sterilization, and preservation*, *4*.
2) Zimmermann, M., & Trumbo, P. R. (2013). Iodine. Advances in Nutrition, 4(2), 262–264.
3) Mebis, L., Langouche, L., & Van den Berghe, G. (2008). Changes within the thyroid axis during the course of critical illness. *Acute Endocrinology: From Cause to Consequence*, 199–213.
4) Wei, X., Luo, C., He, Y., Huang, H., Ran, F., Liao, W., Tan, P., Fan, S., Cheng, Y., & Zhang, D. (2021). Hepatoprotective effects of different extracts from Triphala against CCl4-induced acute liver injury in mice. *Frontiers in Pharmacology*, *12*, 664607.
5) Rose, J., Brian, C., Woods, J., Pappa, A., Panayiotidis, M. I., Powers, R., & Franco, R. (2017). Mitochondrial dysfunction in glial cells: Implications for neuronal homeostasis and survival. *Toxicology*, *391*, 109–115.
6) Feng, X., Chen, A., Zhang, Y., Wang, J., Shao, L., & Wei, L. (2015). Central nervous system toxicity of metallic nanoparticles. *International Journal of Nanomedicine*, 4321–4340.
7) Sree, S., Parkkinen, I., Their, A., Airavaara, M., & Jokitalo, E. (2021). Morphological heterogeneity of the endoplasmic reticulum within neurons and its implications in neurodegeneration. *Cells*, *10*(5), 970.
8) McGurk, S. (2013). Junqueira's Basic Histology Text and Atlas. *Nursing Standard*, *28*(16), 34.
9) Ismail, H. T. H. (2022). The Impact of Iodine Exposure in Excess on Hormonal Aspects and Hemato Biochemical Profile in Rats. *Biological Trace Element Research*, *200*(2), 706–719. https://doi.org/10.1007/s12011-021-02681-7
10) Sauleau, P., Lapouble, E., Val-Laillet, D., & Malbert, C.-H. (2009). The pig model in brain imaging and neurosurgery. *Animal*, *3*(8), 1138–1151.
11) Abdel-Daim, M. M., Shaheen, H. M., Abushouk, A. I., Toraih, E. A., Fawzy, M. S., Alansari, W. S., Aleya, L., & Bungau, S. (2018). Thymoquinone and diallyl sulfide protect against fipronil- induced oxidative injury in rats. *Environmental Science and Pollution Research*, *25*(24), 23909–23916.
12) Jarand, C. W. (2011). *Complexation of Organic Guests and Coordination of Metal Ions by Cyclodextrins: Role of Cyclodextrins in Metal-Guest Interactions*. University of New Orleans.
13) Hoda, S. A., & Hoda, R. S. (2020). *Robbins and cotran pathologic basis of disease*. Oxford University Press US.
14) Maheswari, N., Behera, S., & Mahapatro, A. (2024). Satyashree Ray. A Prospective Observational Study on the Role of Special Stains in Physiological and Histopathological Study of Liver. *Fortune Journal of Health Sciences*, *7*, 192–196.
15) Ippolito, D. L., AbdulHameed, M. D. M., Tawa, G. J., Baer, C. E., Permenter, M. G., McDyre, B. C., Dennis, W. E., Boyle, M. H., Hobbs, C. A., & Streicker, M. A. (2016). Gene expression patterns associated with histopathology in toxic liver fibrosis. *Toxicological Sciences*, *149*(1), 67–88.
16) Czaja, A. J. (2014). Hepatic inflammation and progressive liver fibrosis in chronic liver disease. *World Journal of Gastroenterology: WJG*, *20*(10), 2515.
17) Semenovich, D. S., Andrianova, N. V, Zorova, L. D., Pevzner, I. B., Abramicheva, P. A., Elchaninov, A. V, Markova, O. V, Petrukhina, A. S., Zorov, D. B., & Plotnikov, E. Y. (2023). Fibrosis development linked to alterations in glucose and energy metabolism and prooxidant–antioxidant balance in experimental models of liver injury. *Antioxidants*, *12*(8), 1604.
18) Jarrar, B. M., & Taib, N. T. (2012). Histological and histochemical alterations in the liver induced by lead chronic toxicity. *Saudi Journal of Biological Sciences*, *19*(2), 203–210
19) Ge, Y., Ning, H., Wang, S., & Wang, J. (2005). Effects of high fluoride and low iodine on brain histopathology in offspring rats. *Fluoride*, *38*(2), 127–132.
20) Vadori, V., Peruffo, A., Graïc, J.-M., Vadori, G.,

Finos, L., & Grisan, E. (2024). Revealing cortical layers in histological brain images with self-supervised graph convolutional networks applied to cell-graphs. *2024 IEEE International Symposium on Biomedical Imaging (ISBI)*, 1–5.

21) Chandra, A. K. (2021). Iodine in Disruption of Thyroid and Thyroid Hormone Receptive Systems. *Proceedings of the Zoological Society*, *74*(4), 494–506.

22) Kaufmann, W., Bolon, B., Bradley, A., Butt, M., Czasch, S., Garman, R. H., George, C., Gröters, S., Krinke, G., & Little, P. (2012). Proliferative and nonproliferative lesions of the rat and mouse central and peripheral nervous systems. *Toxicologic Pathology*, *40*(4_suppl), 87S-157S.

23) Yan, J., Iturria-Medina, Y., Bezgin, G., Toussaint, P. J., Xie, K., He, L., Chen, J., Hilger, K., Genç, E., & Evans, A. C. (2026). Comprehensive large-scale analyses reveal association between brain structure and cognitive ability during adolescence. *Communications Biology*.

24) Golubev, A. M. (n.d.). Morphological Classification of Neuronal Damage. *GENERAL REANIMATOLOGY*, 4.

25) Karbownik-Lewińska, M., Stępniak, J., Iwan, P., & Lewiński, A. (2022). Iodine as a potential endocrine disruptor—a role of oxidative stress. *Endocrine*, *78*(2), 219–240. https://doi.org/10.1007/s12020-022-03107-7

26) Basha, P. M., Rai, P., & Begum, S. (2011). Fluoride toxicity and status of serum thyroid hormones, brain histopathology, and learning memory in rats: a multigenerational assessment. *Biological Trace Element Research*, *144*(1), 1083–1094.

27) Mariajoseph, F. P., Lai, L., Moore, J., Chandra, R., Goldschlager, T., Praeger, A. J., & Slater, L.-A. (2024). Pathophysiology of contrast-induced neurotoxicity: a narrative review of possible mechanisms. *European Neurology*, *87*(1), 26–35.

28) Nabi, M., & Tabassum, N. (2022). Role of environmental toxicants on neurodegenerative disorders. *Frontiers in Toxicology*, *4*, 837579.